AD_____

Award Number: W81XWH-10-1-0393

TITLE: Commissioning and characterization of a dedicated high resolution breast PET camera

PRINCIPAL INVESTIGATOR: ArneVandenbroucke,Ph.D.

CONTRACTING ORGANIZATION: Stanford University
Stanford, CA 94305

REPORT DATE: July 2013

TYPE OF REPORT: Annual Summary

PREPARED FOR: U.S. Army Medical Research and Materiel Command
Fort Detrick, Maryland 21702-5012

REPORT DOCUMENTATION PAGE

Form Approved
OMB No. 0704-0188

1. REPORT DATE	**2. REPORT TYPE**	**3. DATES COVERED**
July 2013	Annual Summary	15 June 2012 – 14 June 2013

4. TITLE AND SUBTITLE

Commissioning and characterization of a dedicated high resolution breast PET camera

5a. CONTRACT NUMBER

5b. GRANT NUMBER
W81XWH-10-1-0393

5c. PROGRAM ELEMENT NUMBER

6. AUTHOR(S)

Arne Vandenbroucke

E-Mail: arnevdb@stanford.edu

5d. PROJECT NUMBER

5e. TASK NUMBER

5f. WORK UNIT NUMBER

7. PERFORMING ORGANIZATION NAME(S) AND ADDRESS(ES)

Stanford University
Stanford, CA 94305

8. PERFORMING ORGANIZATION REPORT NUMBER

9. SPONSORING / MONITORING AGENCY NAME(S) AND ADDRESS(ES)
U.S. Army Medical Research and Materiel Command
Fort Detrick, Maryland 21702-5012

10. SPONSOR/MONITOR'S ACRONYM(S)

11. SPONSOR/MONITOR'S REPORT NUMBER(S)

12. DISTRIBUTION / AVAILABILITY STATEMENT
Approved for Public Release; Distribution Unlimited

13. SUPPLEMENTARY NOTES

14. ABSTRACT

The high-resolution breast camera under development for this project consists of many detector modules formed by coupling pairs of high resolution scintillation crystal arrays to position sensitive avalanche photodiodes (PSAPDs). These LYSO crystal arrays contain 64 1mm3 crystal elements. The modules are organized in cartridges built out of 8 layers of 16 modules each. During this funding cycle two cartridges were constructed and operated in coincidence. Intrinsic spatial resolution was determined to be 0.85 mm. Software was written to perform calibration of the subsystem consisting of 512 PSAPDs. A global energy resolution of 10.62 +/ 0.04% FWHM (at 511 keV) was obtained. Reportable outcomes include 2 peer reviewed publications, 2 abstracts submitted to the IEEE NSS-MIC conference, and 3 conference proceedings articles.

15. SUBJECT TERMS
Breast Cancer imaging, high resolution, PET camera

16. SECURITY CLASSIFICATION OF:			**17. LIMITATION OF ABSTRACT**	**18. NUMBER OF PAGES**	**19a. NAME OF RESPONSIBLE PERSON**
a. REPORT	**b. ABSTRACT**	**c. THIS PAGE**			USAMRMC
U	U	U	UU	12	**19b. TELEPHONE NUMBER** *(include area code)*

Contents

1 Introduction

The DOD funded project titled 'Commissioning and Characterization of a Dedicated High-Resolution Breast PET Camera' aims at enhancing the role of PET in breast cancer management by constructing a high resolution PET camera. PET is an imaging modality whereby lesions are visualized based on biochemical activity, rather than lesions' morphology, which is visualized by other imaging modalities such as mammography, MRI, and ultrasound. We will test this high-resolution PET system in the following indications: (1) resolving inconclusive screening mammograms which often show up for patients with dense breasts, (2) enhance staging accuracy, and (3) monitor the response to neo-adjuvant therapy. Dedicated high-resolution cameras can detect smaller lesions and thus enhance the precision of the images. Because of their high sensitivity these cameras can also reduce the injected patient dose. We aim to achieve 1 mm^3 resolution using a unique detector design that is able to measure annihilation radiation coming from the PET tracer in 3 dimensions, using many $1 \times 1 \times 1$ mm^3 scintillation crystals.

2 Body: Research accomplishments as outlined in SOW

2-SA1 Building a block setup: months 1-6

Goal of the first task in this project was to test camera detection concepts, obtain experience working with many channels and perform image reconstruction. We used dual modules that each contain 2 position sensitive avalanche photodiodes (PSAPDs) coupled to 8×8 array of $1 \times 1 \times 1$ mm^3 LYSO crystals. The two PSAPDs are mounted on a thin flexible circuit and are multiplexed as described in [1]. As mentioned in previous year's annual report we completed this task in FY02, due to significant delays caused by a required redesign of the setup due to substantial electromagnetic interference.

2-SA2 Acceptance test of the LSO-PSAPD modules: months 7-15

As reported in FY01 annual report the acceptance testing was delayed due to HV problems. Delivery of 'hot' modules started in the 5th month of FY02 (November 2011). As of July 2013 over 1,200 modules were received of the the total 2400. These modules all went through our acceptance test with an acceptance rate of about 80 %. We are now testing about 2 modules per hour, which is about half as fast as anticipated in the statement of work. The reduced rate is due to the requirement of obtaining calibration data at multiple bias voltages to ensure we are selecting the correct bias voltage. Reference [3] mentions the effects of bias voltage on the PSAPD performance.

The project delay that occured during the first funding year resulted in a delayed module production. RMD Inc., the manufacturer of the dual modules was unable to speed up production and hence the delayed start propagated through the entire project. Currently modules are produced at an average rate of 13.5 per week. Assembly of these modules is a tedious effort.

Since this project is a sequential effort, the aforementioned delay resulted in delay towards all specific aims. Nonetheless we were able to build a significant portion of the camera and study its functionality.

2-SA3 Camera Construction: months 16-26

2-SA3-A Assembly of one panel and testing: months 16-22

During FY03 we managed to fully construct 2 cartridges and operate them in coincidence. Each cartridge consists of 8 layers of 16 modules arranged side-by-side. Each cartridge thus has 128 modules, or 256 PSAPDs. We operated the system with all final electronics and readout paths as intended in the final camera.

The electronics developed and optimized includes (1) the high voltage (HV) board, which distributes HV to each individual module, (2) the signal conditioning board with bias resistors and attenuation circuitry, (3) the RENA board, responsible for charge amplification and digitization and (4) the data acquisition board (DAQ), needed for communication with the computer. All circuit boards are labeled in the photograph on the right panel of Figure 1.

In order to measure the intrinsic spatial resolution of the system with all finalized electronics in place, we measured the point-spread function (PSF) by stepping a radioactive ^{22}Na source across the front face of a crystal array and measure the response of opposing crystal pairs. Doing so we obtained an intrinsic energy resolution of 0.84 ± 0.02 mm, which is below the design goal of 1 mm.

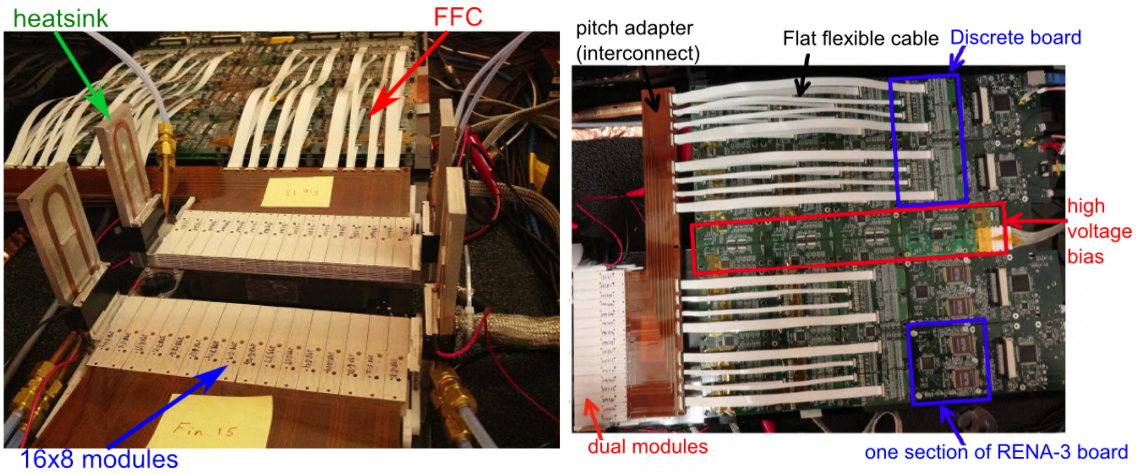

Figure 1: The **left** panel shows a photograph of the completed part of the camera. Two panels with each 8 layers of 16 dual modules can be seen. A water cooled heatsink is visible as well. Flat Flexible Cables (FFC) that lead to the backend electronics are also indicated in the figure. The picture on the **right** shows a top view of one panel. (1) High voltage board, (2) signal conditioning board, (3) RENA board. The data acquisition board (4) is on the rightmost side of the figure. The picture also shows dual modules and FFC interconnects

2-SA3-B Finish construction of the Camera: months 23-26

Due to the delays mentioned in section 2-SA2 we were not able to finish the construction of the camera as a whole. However we did built a significant fraction of the camera. Due to the modular nature of our design, it is expected that adding subsequent cartridges would be straightforward.

In addition to finalizing cartridge assembly and electronics, we also wrote software that programs and reads out the constructed cartridges, and assembly procedures were finalized.

Due to the strong relationship between performance and temperature of a PSAPD [3] (see figure 2, right), it is mandatory to implement thermal regulation in the design. We use aluminum *fins* which the modules are mounted to using a miniature screw. These fins conduct the produced

heat (about 3 mW per fin) to the edge of the detector panels. A thermoelectric (Peltier) element is located at both edges. The hot side of the Peltier element is cooled by a water cooled heat-sink. Each *fin* includes a thermistor for temperature readout so a feedback loop can be established.

The left panel of figure 2 shows a computer drawing of the cooling setup. Using this design, we were able to maintain constant temperature over more than 5 hours, shown by the constant leakage current in 8 modules and a constant thermistor reading in the middle panel of Figure 2. At roughly 18,000 and 25,000 seconds we intentionally increased the temperature by decreasing the current to the Peltier elements. Lowering the water temperature from 20 $^{\circ}C$ to 15° at around t=36,000 s, caused the decrease on the right. Our intent is to maintain the detectors at a constant temperature of 22.0 ± 0.5 $^{\circ}C$.

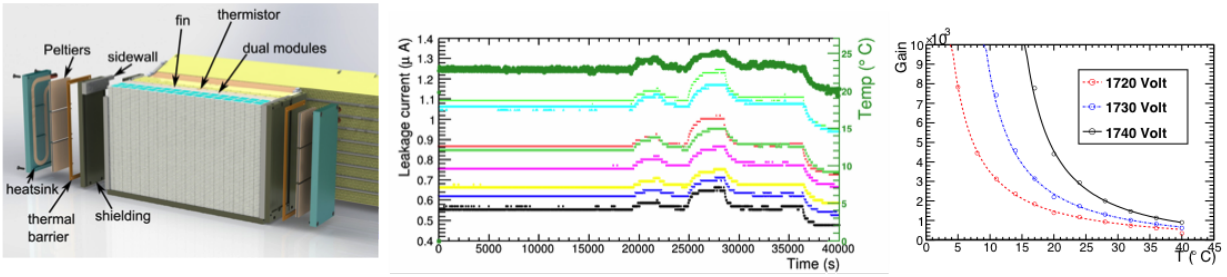

Figure 2: Left Implementation of the cooling in our design. Side-walls, shielding, thermoelectric elements and liquid heat sink are shown in the figure. **Middle:** Measured leakage current for 8 modules in the middle of one of the layers in a cartridge and temperature of the specific layer (thick line, with scale to the right) over time (see text). **Right:** gain as a function of temperature.

2-SA4 Commissioning and Characterization of the Camera: months 27-32

Due to the aforementioned delays we performed commissioning and characterization of the camera with part of the camera only. Nonetheless this study yields important insights in camera performance and commissioning.

Figure 3 shows the energy spectrum of all calibrated crystals in the dual cartridge setup. Data from 444 of 512 (= 87%) crystal arrays/PSAPDs are aggregated in the spectrum shown, with an energy resolution of $10.62 \pm 0.04\%$ FWHM at 511 keV achieved. The Lu X-ray escape peak (at about 450 keV) is visible as a hump on the left side of the photopeak, indicating excellent system energy resolution. The bottom panel of the figure shows the distribution of energy resolution for 444 LYSO-PSAPD detectors in the setup. The distribution is centered around 10.2%, with only a few outliers (< 1 %) towards worse energy resolution.

In order to achieve good timing resolution, we need to correct for at least three factors: (1) different signal path lengths depending on the location of the RENA-3 chip in the system, (2) different signal arrival times dependent on the crystal location on the PSAPD surface, due to the different RC-constant encountered, and (3) trigger walk, i.e. dependence of trigger time on signal amplitude. The 2nd factor is indicated on the bottom of Figure 8. We see that a difference in arrival time of up to 20 ns is observed between center and edge crystals. We created calibration software that takes these three factors into account. The result is an overall coincidence time resolution of 12.2 ± 0.2 ns FWHM shown on the left of Figure 4. The humps on the right and left of the peak correspond to inter-array scatter events: for these events the timing calibration will be off, as the software will assume a wrong location for the interaction. It is important to stress that the coincidence time resolution shown was obtained using the 444 LYSO-PSAPD detectors from

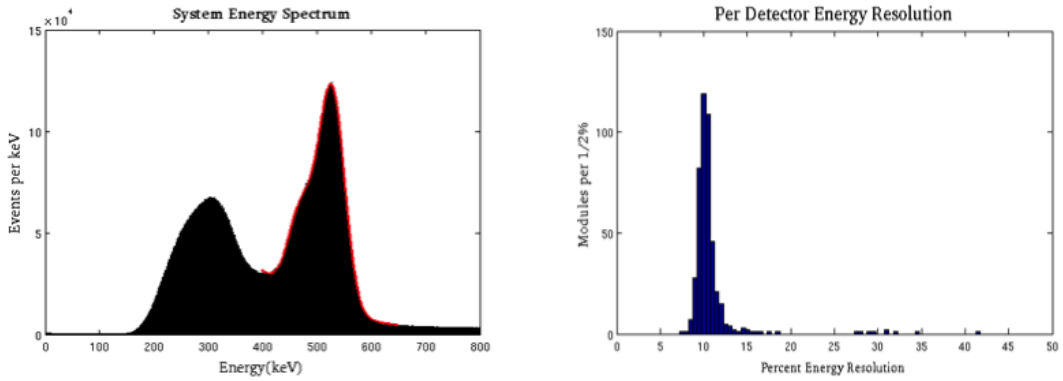

Figure 3: Left: Global, calibrated energy spectrum of all crystals in the system is 10.62% FWHM. **Right:** the distribution of all energy resolutions per crystal. Data shown are aggregated from 444 LYSO-PSAPD dual-modules in the system.

the two cartridge system setup, including all interconnects, circuit boards, 64 RENA-3 chips (with leading edge discriminator) and power supply lines.

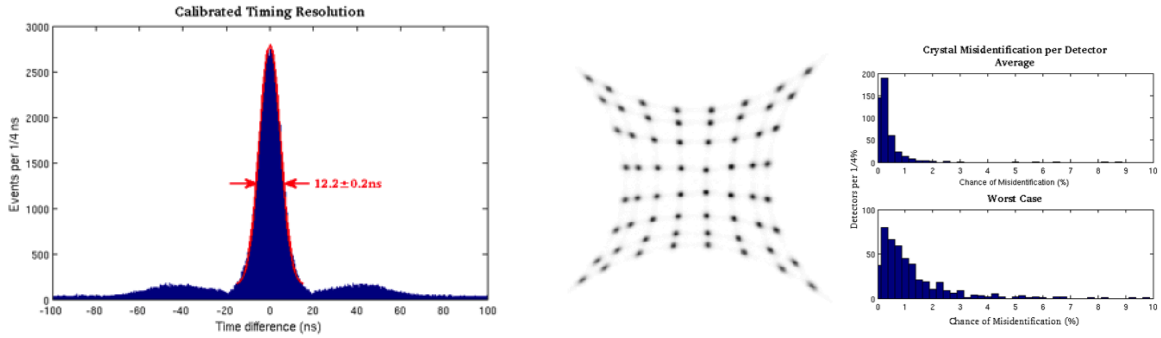

Figure 4: Left: System coincidence timing resolution of 12.2 ns FWHM. **Middle:** Flood histogram aggregated over 444 LYSO-PSAPD detectors in the two cartridge setup. **Right:** Misidentification probability of assigning events to 1 mm crystal elements averaged over each array (top) and for the poorest identified crystal (bottom), for 444 crystal arrays.

The right panel of Figure 4 shows a system flood histogram aggregated over 444 LYSO-PSAPD detectors, as obtained in the two-cartridge system setup. We have implemented algorithms that segment and sort all crystals in the flood histogram. In order to assign misidentification probabilities, we analyzed the overlap of fitted Gaussian functions to the peaks in the row-by-row projection of the flood histogram. The top right panel of the figure shows the average misidentification probabilities for each array. The vast majority of the arrays have less than 1% misidentification. The bottom right shows the worst case: in general the crystals at the edge have worse separation due to the reduced gain at the edges of the PSAPD in each array. The bulk of the data shows less than 2% misidentification probability, a consequence of the very high scintillation light collection aspect ratio in our design (enabling well-separated crystals in flood image), the use of intercrystal reflectors, and good signal-to-noise ratio (SNR).

Spatial resolution (point spread function (PSF)) was measured by stepping a 0.25 μm point source in 100 μm steps across the face of the two opposing cartridges, and counting the coincidence

events in opposing crystal pairs. Doing so, the PSF is obtained, which was measured to be 0.84±0.02 mm on average, again using all electronics and interconnects to be used in the final system. The left panel of figure 5 shows the PSF across two opposing crystal arrays (one from each of the two cartridges). The 8 central peaks correspond to all 8 crystals in an array row. The peaks on the left and right correspond to the first crystals on neighboring arrays. The 2.87 mm gap between arrays is also visible.

To characterize imaging performance using the two-cartridge PET system, we imaged a micro-Derenzo phantom (figure 5, middle panel), the results of which are shown on the right of figure 5. A GPU implementation of List-mode Maximum Likelihood expectation maximization (MLEM) was used to reconstruct the image. The MLEM statistical model incorporated geometric effects, such as scanner asymmetry, inter-detector gaps, LOR geometry and non-uniform detection efficiencies. The latter normalization coefficients were measured by acquiring a uniform calibration phantom. Random coincidences were addressed via the delayed coincidence window method. Although we only used a small subset of the final system (i.e. small number of counts) and non-optimal normalization code, the 1.6 mm spheres are distinctly visible.

A No-Cost Extension (NCE) has been requested for this project. During this NCE, we will increase the resolution of reconstructed images by exploring improved DAQ software and refined normalization and calibration algorithms, as well as improved random and scatter corrections. The goal is to be able to resolve at least the 1.2 mm rods.

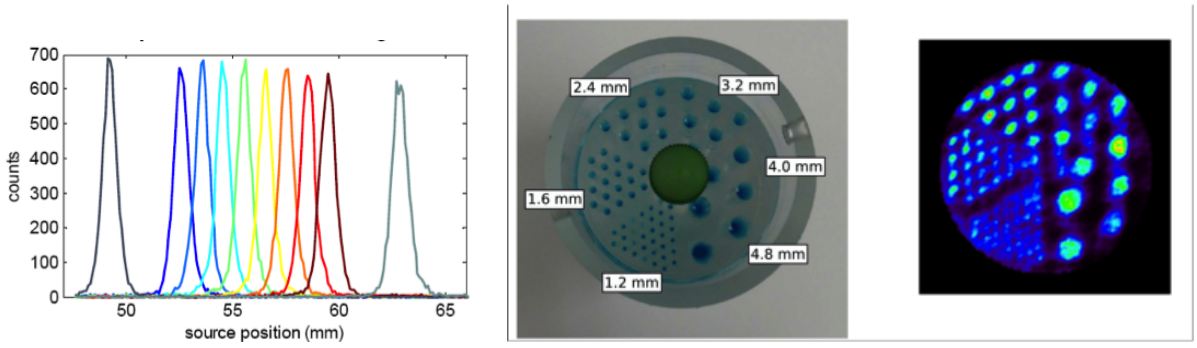

Figure 5: Left: Coincidence point spread function (PSF) measured across an array of the two-cartridge system shown in 1. **Middle:** Photograph and **Right:** Reconstructed image of the micro-Derenzo phantom acquired by the two-cartridge system with 6 cm panel separation. The orientation of the phantom was orthogonal to the two detector cartridges, so the image includes non-isotropic resolution artifacts inherent to the limited angle tomography geometry.

2-SA5 Prepare patient studies: months 33-36

Due to the aforementioned delays, patient studies could not be prepared. However, we met several times with Dr. Ikeda, head of the Stanford Breast Imaging Center, and with Dr. Wapnir, Chief of Breast Surgery at Stanford to outline the first studies with this camera. Consensus was to aim at two pilot studies. For Pilot Study I, 10 patient will be recruited that are undergoing a regular staging PET/CT. We will image with the novel two-panel system after the standard PET/CT scan, in order not to interfere with the standard practice of care. In addition, we won't need to administer FDG for the sole purpose of the study: we will image with the remainder of the activity. This study will allow us to compare performance of our camera with standard PET/CT imaging devices, albeit at an effective lower dose. We will evaluate and compare lesion size, contrast and

standard uptake value (SUV).

Pilot Study II will validate the utility of 1 mm^3 resolution breast-dedicated PET in 10 women with newly diagnosed breast cancer who harbor other lesions in either breast that will be biopsied. Preferably these patients will have had an MRI scan so we can compare outcome of our system with the results of an MRI system and pathology.

3 Key Research Accomplishments

- Constructed two cartridges and operated them in coincidence. The setup includes 512 PSAPDs, each biased at around 1750 Volts.
- We verified an intrinsic spatial resolution of 0.84 ± 0.02 mm.
- We determined a **system-wide** energy resolution of 10.62 ± 0.04 % FWHM, a coincidence time resolution of 12.2 ± 0.2 ns, and an average misidentification rate of < 1 %.
- For the first time, we were able to acquire and reconstruct a micro-Derenzo phantom with this setup.
- About 45 % of the modules to be used in the final system are tested and 80 % of those are accepted.

4 Reportable Outcomes

4.1 Abstracts

- Abstracts submitted and accepted to the 2013 *IEEE Nuclear Science Symposium and Medical Imaging Conference*, to be held October 2013, Seoul, Korea:

    1. A. Vandenbroucke, P. D. Reynolds, F. W. Lau, D. Innes, A. Mihlin, D. L. Freese, D. F. Hsu, C. S. Levin: *First Measurements of a 512 PSAPD Prototype of a Sub-MM Resolution Clinical PET Camera*
    2. D. L. Freese, A. Vandenbroucke, D. Innes, F. W. Y. Lau, D. Hsu, P. D. Reynolds, C. S. Levin: *Current and Temperature monitoring and thermal regulation performance of a clinical PET system consisting of many APDs*
    3. S. Cui, A. Vandenbroucke, M. Bieniosek, and C.S. Levin: *General spatial distortion correction method for solid-state position sensitive detectors in PET*

4.2 Publications

1. A. Vandenbroucke, T.J. McLaughlin, C.S. Levin Performance evaluation of a large area position sensitive avalanche photodiode coupled to an LSO crystal array as a function of temperature and bias voltage *J. Inst* **7**, P08001, Aug 2012.

2. F. W. Y. Lau, A. Vandenbroucke, P. Reynolds, H. Ho, D. Innes, and C. S. Levin, Signal Conditioning Technique for Position Sensitive Photodetectors to Manipulate Pixelated Crystal Identification Capabilities, IEEE Transactions on Nuclear Science, vol. 59, no. 5, pp. 1815-1822, 2012.

4.3 Conference Records

1. P.D. Reynolds, F.W.Y. Lau, A. Vandenbroucke, D. Innes, U. Yoruk, C.S. Levin, Characterization of detector layers from a 1 mm3 resolution clinical PET system *Nuc. Sci. Conf. Rec.* **2012**, 3804-3807

2. U. Yoruk, A. Vandenbroucke, P.D. Reynolds, C.S. Levin, Design and implementation of scalable DAQ software for a high-resolution PET camera *Nuc. Sci. Conf. Rec.* **2012**, 2537-2539

3. F.W.Y. Lau, J.Y. Yeom, A. Vandenbroucke, P.D. Reynolds, D. Innes, C.S. Levin, A cost-effective modular programmable HV distribution system for photodetectors *Nuc. Sci. Conf. Rec.* **2012**, 3504-3506

4.4 Book Chapter

1. A. Vandenbroucke, C.S. Levin *Engineering the next generation PET detectors*, to be published in *Engineering in Translational Medicine*, edited by W. Cai, Springer, 2013

5 Conclusions

Significant progress towards completion of the 1 mm^3 resolution breast specific PET camera was made during the third funding year. We have received about 45 % of the modules and about 80 % of these passed our functionality criteria. We managed to construct 2 cartridges, with 256 dual modules each. We connected these to the readout electronics that we will use in the final system.

We constructed two cartridges, including the finalized signal conditioning and readout electronics, as well as the high voltage biasing circuitry. A global energy resolutions of 10.62 ± 0.04 % FWHM was obtained for the entire system. A global coincidence time resolution of 12.2 ± 0.2 ns FWHM was measured.

Commissioning two cartridges operating in coincidence is major progress. All cartridges in the camera operate independently, so adding more cartridges should be relatively straightforward. We anticipate to copy assembly procedures and readout electronics when adding more cartridges.

We measured an intrinsic spatial resolution of 0.84 ± 0.02 mm, which is below the design goal of 1 mm. This high spatial resolution is partly due to a low average misidentification rate of < 1 %.

Despite significant project delay, the reported results show that we made good progress towards construction of the breast dedicated PET camera described in the project. We have overcome significant technical problems. We plan to test the $1mm^3$ resolution PET camera to assist in breast cancer management by resolving inconclusive mammograms, performing local staging and analyzing response to therapy.

References

[1] Lau F W Y, Vandenbroucke A, Reynolds P D, Olcott P D et al. 2010 Analog signal multiplexing for PSAPD-based PET detectors: simulation and experimental validation *Phys. Med. Biol.* **55**, 7149.

[2] A. Vandenbroucke, F.W.Y. Lau, P.D. Reynolds, C.S. Levin: *Measuring 511 keV Photon Interaction Locations in Three Dimensional Position Sensitive Scintillation Detectors Nuc. Sci. Conf. Rec* **2011**, p 3635-3638

[3] A. Vandenbroucke, T.J. McLaughlin, C.S. Levin Performance evaluation of a large area position sensitive avalanche photodiode coupled to an LSO crystal array as a function of temperature and bias voltage *J. Inst* **7**, P08001

[4] F.W.Y Lau, A. Vandenbroucke, P.D. Reynolds, H. Ho, D. Innes, C.S. Levin Signal Conditioning Technique for Position Sensitive Photodetectors to Manipulate Pixelated Crystal Identification Capabilities *Trans. Nucl. Sci*, accepted for publication

[5] J. Zhai, A. Vandenbroucke, P.D. Reynolds, C.S. Levin Functionality Test of a Readout Circuit for a $1mm^3$ Resolution Clinical PET System, *Nuc. Sci. Conf. Rec* **2012**, p 3945-3949